THE ASTROPHYSICAL JOURNAL, 298:596–613, 1985 November 15

KINEMATICS OF THE H II REGION SHARPLESS 142. II. RADIO CONTINUUM AND LINE (21 CENTIMETER) OBSERVATIONS

G. JONCAS,[1,2] P. E. DEWDNEY,[3] L. A. HIGGS,[3] AND J. R. ROY[1]

Received 1985 January 17; accepted 1985 April 15

ABSTRACT

We present 21 cm aperture synthesis observations of the continuum and H I line emission of a 2° field centered on the H II region S142. The resolution is $1' \times 1'.1 \times 1.3$ km s^{-1} in radial velocity. Both line and continuum maps contain all spatial information out to a $2400\lambda \times 2800\lambda$ elliptical boundary in the u-v plane. A list of background radio sources in this field is presented along with a detailed analysis of S142.

The thermal continuum emission from S142 has an extent of $42' \times 23'$. The emission falls off sharply on the east side but fans out in a large region of low intensity in other directions. The total continuum flux is 13.3 Jy, and the peak emission measure is 15,800 cm^{-6} pc. A simple model of the ionized gas density distribution yields a total ionized mass of 4000 $M_\odot$.

The H I emission in the region around S142 has a complicated structure, typical of regions near the Galactic plane. Several H I emission features related to S142, forming a partial shell around the H II region, appear to be gas which has been dissociated by the exciting star. The total mass of H I, $\sim$3000 $M_\odot$, greatly exceeds the mass of molecular material present ($\sim$200 $M_\odot$).

DH Cep, the exciting star, is contained in a young open cluster, NGC 7380. We interpret the present scene in the cluster/gas complex as having resulted from (low-mass) star formation which was terminated by the formation of DH Cep. This star is now in the last stages of dispersing the progenitor cloud.

Subject headings: clusters: open — nebulae: H II regions — nebulae: individual — radio sources: 21 cm radiation — stars: individual

I. INTRODUCTION

An understanding of the interaction of H II regions with their surroundings is important because of its relevance to the distribution and dynamics of interstellar matter (both molecular and atomic) as well as star formation. This emphasis requires observations which provide links between the stars, the ionized gas, the atomic gas, and the molecular gas for a wide range of stellar types, densities, and ages.

To the list of H II regions studied in detail, we have added S142, a large H II region in Cepheus situated in the Perseus arm ($l = 107°.1$, $b = -0°.96$). In Joncas and Roy (1984, hereafter Paper I) Hα measurements of the velocity field of the ionized gas in S142 were presented. In this paper we present radio observations of the continuum radiation from S142 itself, and H I line observations of the region around S142. Observations of CO by Israel (1980) complement the other two sets of observations, allowing us to study the H_2–H I–H II complex as a whole. A summary of previous optical and radio emission-line studies of S142 has been given in Paper I. In this paper we will include the background necessary to complete the radio picture, and to bring together the available information relevant to the interaction of stars and gas in this region.

S142 has been detected in a number of radio surveys. The 21 cm survey of Felli and Churchwell (1972) yielded a flux of 12 Jy, and at 73.5 cm Felli *et al.* (1977) measured 17.1 Jy using the east-west arm of the Bologna Cross telescope. The measured low-frequency flux confirms that the source is completely thermal in origin. It is also included in the surveys of Felli *et al.* (1978), Warner and Black (1978), both at 4995 MHz, and Kallas and Reich (1980) at 21 cm.

A 21 cm synthesis map obtained by Israel (1977) has delineated the fine structure of S142, showing that only about 200–300 mJy (a few percent of the total flux) is contained in structure of the order of 0.5 pc or less in size.

Israel (1980) has also made CO observations of the region around S142, discovering a small cloud near the eastern edge. The relationship of this cloud with the H II region and its surroundings will be discussed later in this paper.

Turner (1969) has included S142 in a survey of OH in the Galactic plane without detecting any evidence of an OH maser. No known search for H_2O masers has been made.

Radio recombination-line measurements have been made by Pedlar (1980) (H166α) and by Garay and Rodríguez (1983) (H125α). An electron temperature of 4900 K was derived by Pedlar, using observations made with a 36′ beam, while Garay and Rodríguez obtained 7700 K, using observations made with a 10′ beam centered near the middle of the nebula. The disparity between these two sets of observations may be significant, and confirming observations would be helpful. We assume an electron temperature of 8000 K in this paper.

S142 contains the open cluster, NGC 7380. Moffat (1971) has made photometric measurements of its member stars, giving a distance determination of 3.6 kpc and an age estimate of 2×10^6 yr, based on the upper main sequence in the color-magnitude diagrams. This distance corresponds to a velocity of -40 km s^{-1} in a Schmidt model of the galaxy or to -33 km s^{-1} in a flat rotation curve model outside the solar circle ($V_{\rm Sun} = 250$ km s^{-1}; $R_{\rm Sun} = 10$ kpc). The cluster contains up to 192 stars (Baade 1983) of which three are O-type stars. The ionization of S142 is principally due to HD 215835 (DH Cep),

[1] Département de physique and Observatoire Astronomique du Mont Mégantic, Université Laval.
[2] Observatoire de Marseille.
[3] Dominion Radio Astrophysical Observatory, Herzberg Institute of Astrophysics, National Research Council of Canada.

TABLE 1

OBSERVATIONAL PARAMETERS

Parameter	Value
Observational phase center	$\alpha = 22^h46^m00^s.0$, $\delta = 57°48'00''$ ($l = 107°.187$, $b = -0°.984$)
Primary field pattern	FWHM = 103′ circular
Synthesized beam	FWHM = 1′.0 EW × 1′.1 NS
Polarization	Left circular
Continuum channel sensitivity	ΔS = 0.8 mJy per beam area at map center (1 σ)
Spectral channel sensitivity	ΔT_b = 7 K at map center (1 σ)
Radial velocity resolution	ΔV = 1.32 km s^{-1}
Range in V_{LSR} (128 channels)	+7.7 km s^{-1} to −96.9 km s^{-1} (interferometer); −25.2 km s^{-1} to −75.7 km s^{-1} (single antenna)

the dominant member of the cluster. DH Cep is a spectroscopic eclipsing binary, both components of which have spectral type O6 V (Humphreys 1978). The other two O stars are of type O9 and O9.5 and may both be spectroscopic binaries (Moffat 1971).

II. OBSERVATIONS

a) *Interferometer*

The aperture synthesis radio telescope of the Dominion Radio Astrophysical Observatory consists of (two movable and two fixed) 9 m paraboloids aligned on a 600 m east-west baseline. It is designed to make H I spectral line observations simultaneously with observations of 21 cm continuum emission, uncontaminated with H I emission. Line emission is detected with a digital correlation spectrometer; continuum emission is detected in a 20 MHz band from which the central 5 MHz containing line emission is removed. Observational parameters are listed in Table 1.

Observations were recorded along concentric elliptical tracks in the (u, v) plane, each 12 hr long. Each track was inidividually calibrated for gain and phase using the unresolved calibration sources 3C 295 and 3C 147 with flux densities from Baars *et al.* (1977).

b) *Single Antenna*

Measurements corresponding to the center of the (u, v) plane (not measurable with the DRAO interferometer) were taken from single-antenna observations of the S142 field. For the continuum, the Galactic plane survey of Kallas and Reich (1980), using the 100 m antenna at Effelsberg, was used to fill in the central 71λ of the (u, v) plane. For the H I line, an observation was obtained with the DRAO 26 m paraboloid. Maps of the S142 field were made using frequency switching to subtract instrumental baseline and out-of-band continuum and were calibrated in intensity using the standard regions S6 and S8 (Williams 1973). However, these maps were available over only the central half of the velocity range of the interferometer maps so that full (u, v) coverage exists only for half of the H I maps.

c) *Map Synthesis*

The interferometer observations were interpolated onto a rectangular (u, v) grid and Fourier transformed to make maps in the continuum and in each spectral channel. The continuum map was subtracted from each spectral line map, effectively setting the zero point at the level of the out-of-band continuum. The interferometer maps were scaled to units of brightness temperature using the effective area of the synthesized beam and were then corrected for the primary pattern of the 9 m paraboloids. Maps made with the single antenna were filtered to retain only data at the spatial frequencies missing from the interferometer maps. These maps, calibrated separately, were added to the maps made from the interferometer observations.

III. RADIO CONTINUUM EMISSION

a) *S142*

Figure 1 shows the map of 21 cm continuum emission from a 75′ square field containing S142. The outer boundary of S142 can be traced at the 2 K contour level, and at that level S142 is about 42′ × 23′ in extent, elongated along a northeast-southwest line. At the half-intensity level, the radio emission is about 14′ × 6′ in extent. The emission falls off sharply on the east side but fans out in a large region of low intensity in other directions. There are two peaks of emission with brightness temperatures of 28 ± 1.3 K and 23 ± 1.3 K, respectively (1 σ errors will be used throughout this paper), falling to about 18 K between them. Two other features worth noting are the broad extension to the southwest, and a less prominent extension to the west with a region between them of decreased emission. The emission measures corresponding to the two peaks are 15,800 cm^{-6} pc and 13,400 cm^{-6} pc respectively, assuming an electron temperature of 8000 K.

The total 21 cm continuum flux of S142 is found to be 13.3 ± 0.8 Jy in good agreement with single-antenna measurements (Felli and Churchwell 1972). Using this flux, an electron temperature of 8000 K, and an adopted distance of 3.5 kpc, an excitation parameter of 71 pc cm^{-2} is required, corresponding to 1.4×10^{49} Lyman continuum photons s^{-1}. The uncertainties of the input parameters make the last value inaccurate by about 8%. The principal ionizing star, HD 215835, produces about 3.5×10^{49} photons s^{-1} (Panagia 1973) and is situated on the west side of the H II region at a projected distance of about 9.1 pc from the peak emission. Even considering the offset location of the ionizing star (implying a loss of ionizing photons to the west), there are clearly a sufficient number to maintain the H II region. The two other early-type stars may contribute slightly to the ionization. Their contribution is discussed below.

There is general correspondence in the large-scale structure between optical Hα emission and radio continuum emission (Fig. 2). Both have well-defined eastern boundaries, and both fall off more gradually in other directions. The radio emission shows a larger extent than the Hα emission, owing at least in part to a lesser "equivalent" integration time used for the latter, especially for the southwestern image in the Hα mosaic which has a shorter exposure time than used for the rest of the

mosaic. Inspection of the overexposed picture of S142 in the red print of the Palomar Sky Survey shows a larger extent for the ionized gas. An interesting large-scale feature is a weak trough in the radio emission cutting into the western part of the nebula coincident with a similar trough in Hα emission. This indicates a real deficit of ionized gas in this region.

However, there is little correspondence in the small-scale structure between optical and radio emission, mainly as a result of obscuration by bands of dust which appear to penetrate from the east. In particular, both radio continuum peaks are in obscured regions. There are, however, two exceptions. One is an enhancement of radio emission of about 2 K associated with an Hα knot (Fig. 2) around one of the stars in NGC 7380 (LS III 57°.89). The other is the secondary peak in the radio map which lies partly over the southern bright rim (BS) identified in Paper I. The northern bright rim may have a radio counterpart, but the case is not clear since it lies near the steep eastern boundary of the radio emission. Most of the small-scale optical features in the eastern part of the nebula are probably foreground structures, not associated with the core of

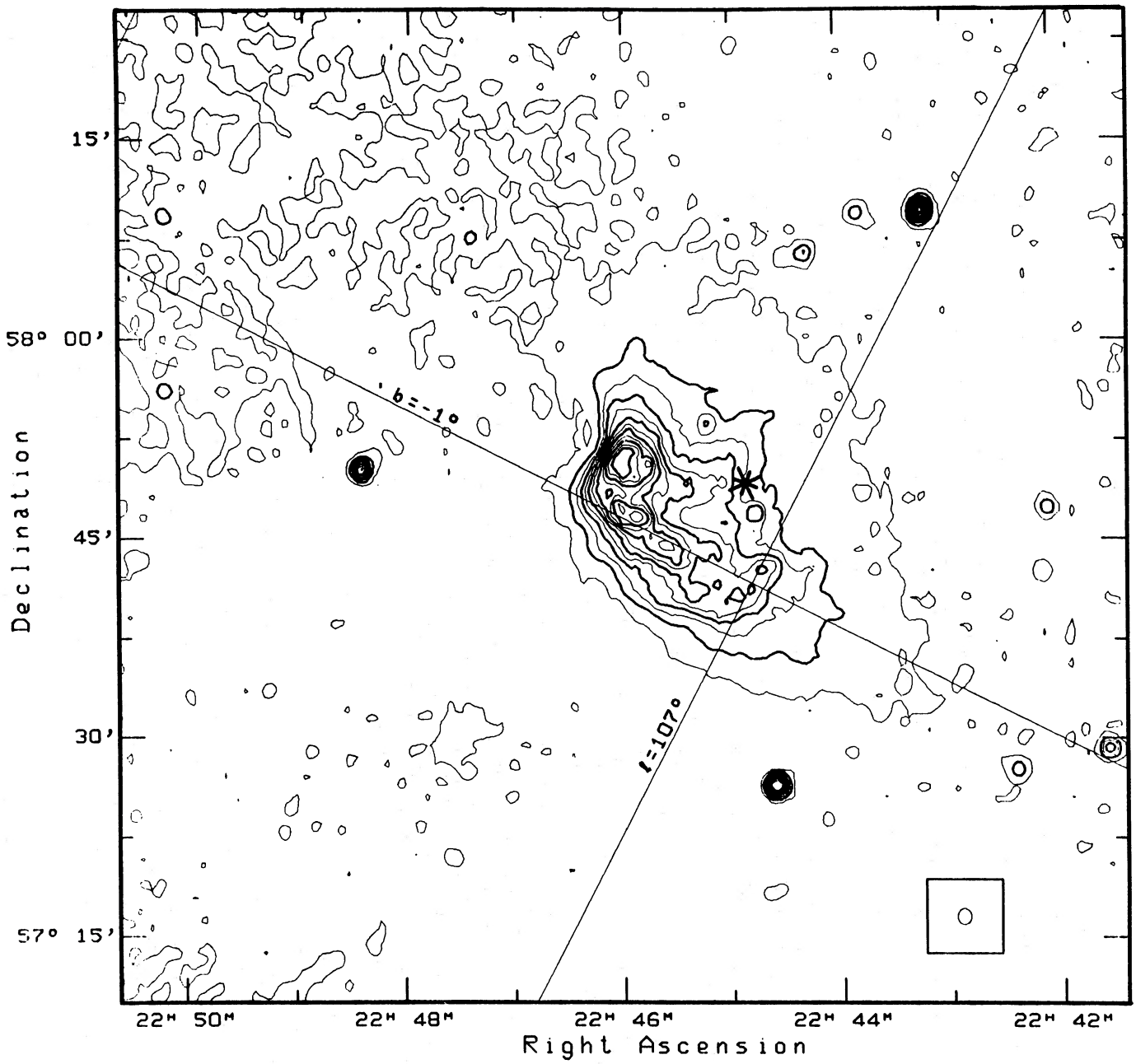

FIG. 1.—The 21 cm map of S142 with a half-power beamwidth of 1'.12 × 0'.98, shown in the lower right corner. The contours are evenly spaced, with a brightness temperature interval of 2 K, starting at 2 K. The peak brightness temperature is 28 K. The main ionizing star of S142 (DH Cep) is shown by the star symbol. The radio emission from S143 is also shown ($\alpha = 22^h47^m.6$; $\delta = 57°30'$). At a distance of 3.5 kpc, 1' is equivalent to 1.02 pc.

FIG. 2.—The map from Fig. 1 with the same contours overlaid on the photographic mosaic in Hα made by Joncas and Roy (Paper I). Features of interest are marked as follows: (a) DH Cep; (b) LS III 57°.83, an O9.5 star; (c) LS III 57°.90, an O9 star; (d) an Hα knot corresponding in position to LS III 57°.89; (e) A bright rim (BN); and (f) A bright rim (BS). Although it may be difficult to see against the white part of the photograph, there is a contour of radio emission around the Hα knot.

the nebula which is largely obscured. The bright rims may be associated with the O9 stars (Paper I).

The large-scale Hα velocity structure (see Figs. 7*a* and 7*b* in Paper I), consists mainly of an increase of radial flow from east to west and away from the observer. The velocity falls off at a mean rate of approximately 2.0 km s^{-1} per projected parsec out to a radius of about 20 pc at all position angles from 180° to 360° centered on the continuum peak, except at 270° where the slope is 1.5 km s^{-1} per projected parsec. Beyond the 20 pc radius in the southwest, the velocity tends to level off. The velocity near the continuum peak is -50 to -60 km s^{-1}, blueshifted by about 15 km s^{-1} from the velocity of the adjacent peak of the CO cloud.

The general shape of the radio map (emission measure), the total radio flux, and the radial falloff in the velocity of ionized gas is adequately modeled by a broad truncated elliptical cone (opening angles of 120° in position angle and 30° in line of sight) of ionized gas tilted about 45° into the plane of the sky

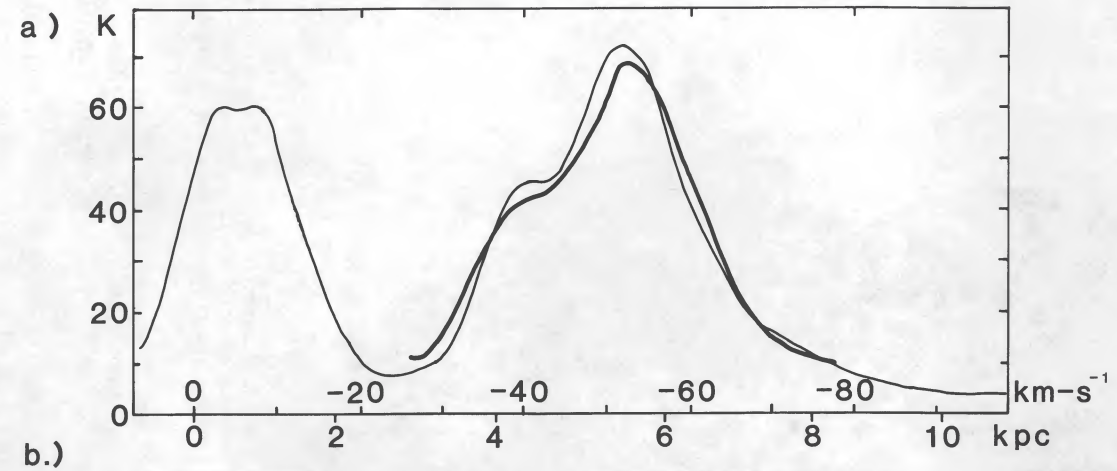

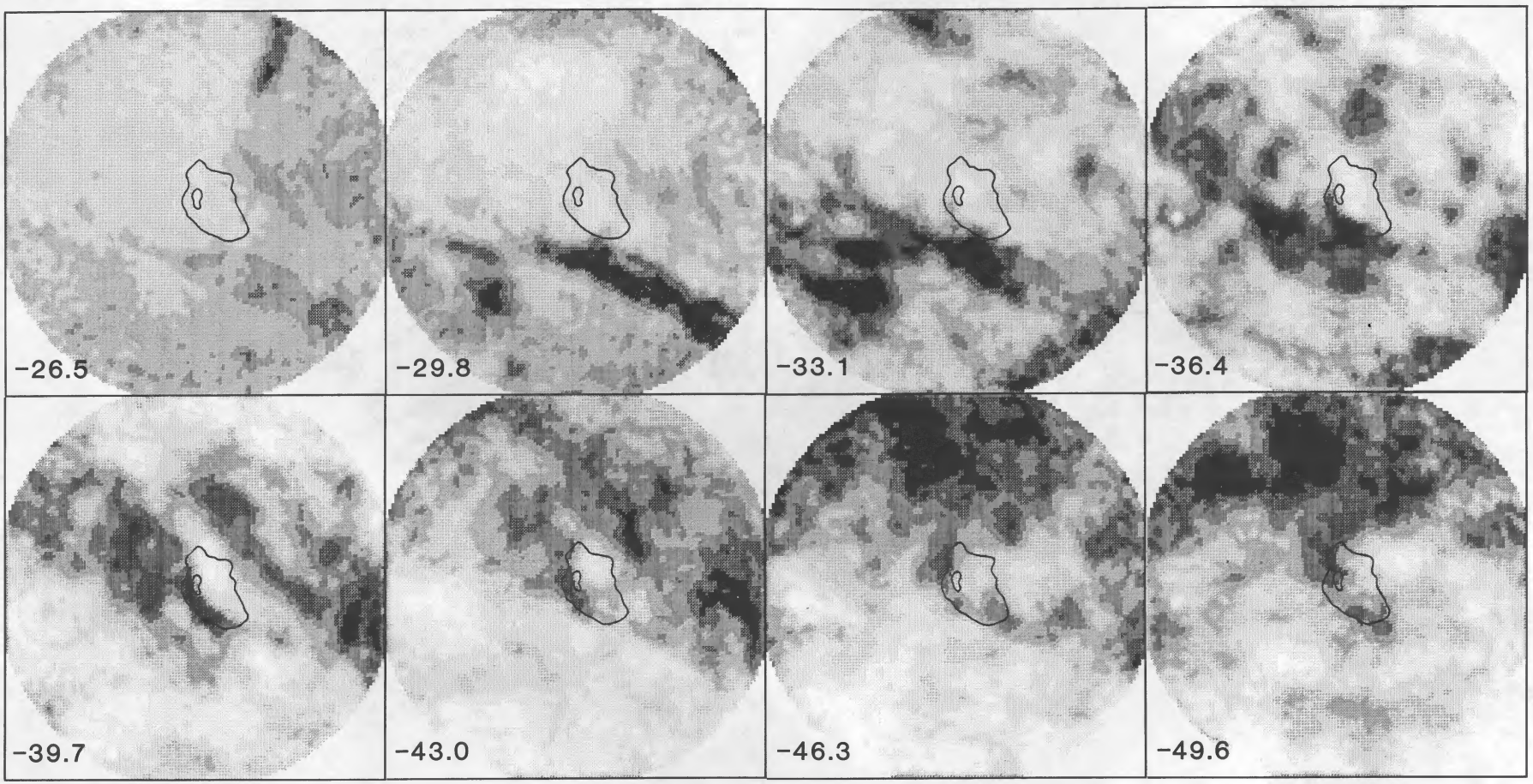

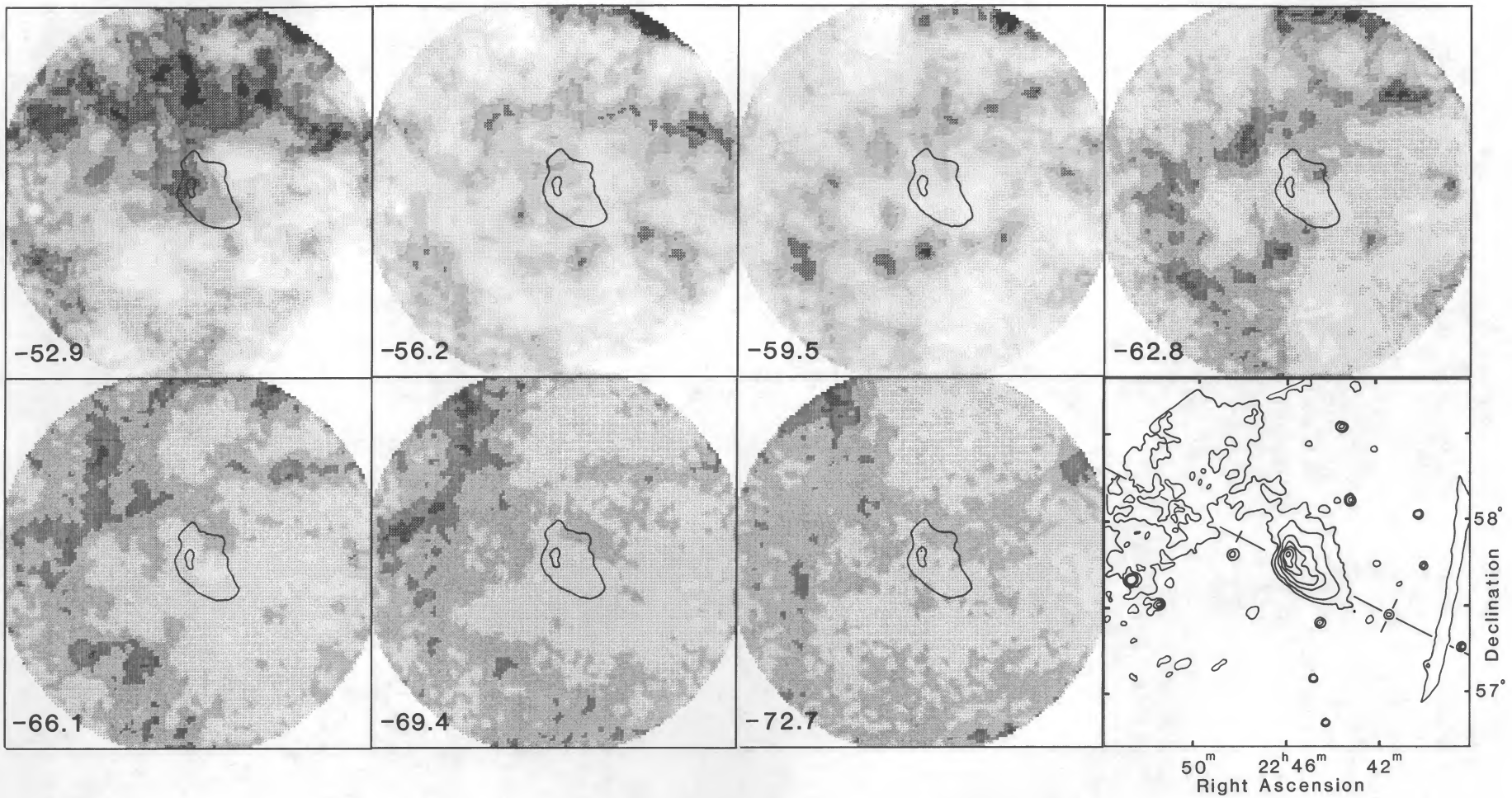

FIG. 3b—*Continued*

FIG. 3.—(*a*) A plot of large-scale H I line emission vs. velocity showing the range of velocities covered by the observations made with the DRAO 26 m paraboloid (-25.2 to -75.5 km s^{-1}), and the range covered by the interferometer observations (7.7 to -90.9 km s^{-1}). The spectrum covering the smaller velocity range is the base spectrum for all the H I maps shown in this paper. H I maps are shown as deviations from the base level corresponding to their particular velocity. The spectrum covering the larger velocity range is from the Weaver and Williams (1973) survey, representing the point at $l = 107.^{\circ}5$ and $b = -1^{\circ}$. The two spectra cannot be compared precisely since the Weaver and Williams spectrum is in antenna temperature units. Also shown is a corresponding distance scale according to a model of the Galaxy with a flat rotation curve ($V_{\odot} = 250$ km s^{-1}, $R_{\odot} = 10$ kpc). (*b*) Maps of H I line (minus out-of-band continuum) emission over a 2° field centered on S142 as well as a matching map of continuum emission. All maps have a spatial resolution of 3′ (FWHM). The line maps are at velocity intervals of 3.3 km s^{-1}. Each of the line maps has had a different base level substracted from it corresponding to the spectrum shown above. There are seven gray levels in the maps: -18, -12, -6, 0, 6, 12, and 18 K respectively. The gray contour interval, 6 K, corresponds to $N = 3.6 \times 10^{18}$ cm^{-2}. The overlaid contours are continuum emission at the 3 K and 18 K levels, respectively. The continuum map at lower right has contour levels of 2, 3, 4, 8, 12, 16, and 20 K. The linear artifact on the right side of this map is a grating lobe of Cas A. The line passing through S142 is at $b = -1^{\circ}$. The tick marks on the line are at $l = 106.^{\circ}5$ and $l = 107.^{\circ}5$.

with a spherical truncation boundary about 5 pc from the apex of the cone. With a peak density of 65 cm^{-3} and a scale height of 12 pc, the density distribution in this model is of the form, $n_e = 65e^{-(R-5)/12}$ cm^{-3}, and the velocity distribution radially away from the truncation boundary is of the form, $V = 10 + 1.4(R - 5)$ km s^{-1}, where R is the radius from the apex of the cone. Conservation of mass requires that ionization at the walls of the cone near the truncation boundary must contribute most of the flowing material, but there is a small contribution from the truncation boundary itself. The derived total mass of ionized material is about 4000 $M_\odot$ (assuming no clumping; see Roy and Joncas 1985), and the derived ionization rate is 0.01 $M_\odot$ yr^{-1}. This model does not explain the blueshifted velocities near the continuum peak. However, not only is the flow likely to be complicated in that region, but also the measurements of Hα emission may not give a true picture because of obscuration.

b) Other Continuum Sources

Figure 1 also contains the first identified radio detection of S143, a small H II region ($V_{LSR} = -25.5$ km s^{-1} at Hα; Georgelin 1985) southeast of S142. The exciting star of S143 has been identified by Georgelin (1975) as LS III 57°.93, an O9.5 V star at a distance of 3.7 kpc. The total flux of this source is 26 mJy, and its peak brightness temperature is 1.3 K, giving an excitation parameter of about 9.1 (assuming an electron temperature of 8000 K) and a peak emission measure of 770 cm^{-6} pc. Comparing the value found for the excitation parameter with the spectral type of the exciting star, S143 seems at least partly density bounded. No CO emission has been detected so far from this nebula (Blitz, Fich, and Stark 1982). S143 also appears on the 6 cm catalog of Taylor and Gregory (1983) as a 80 mJy source. Although part of feature A (described in the next section) overlaps S143, no evidence for H I emission connected with S143 appears in our data.

Table 2 gives a list of other small-diameter sources found in the S142 field, with flux densities greater than 25 mJy, plus a few others. The flux densities, sizes, and position angles corrected for the synthesized beam, have been estimated from fitted Gaussians. In keeping with the system of numbering sources observed with the DRAO synthesis telescope, these sources should be referenced by 7P*n*, where *n* is the serial number in Table 2.

IV. H I LINE EMISSION

For the purpose of displaying the basic H I observations, adjacent line channels were averaged and the resulting maps smoothed to produce a sequence of maps over a 2° field with a 3′ × 3′ spatial resolution and 3.3 km s^{-1} velocity separation. Figure 3*b* shows a subset of 15 of these maps (line minus out-of-band continuum) along with a matching continuum map. As indicated in Figure 3*a*, the velocity of the S142 complex (taken to be the LSR velocity of the ^{12}CO cloud, -41 km s^{-1}) corresponds well to that expected for simple models of Galactic rotation. The H I spectrum from the survey by Weaver and Williams (1973) indicates that S142 lies in the "Perseus arm" of the Galaxy. Although S142 lies at $b = -1°$, the bulk of the galactic H I emission in this direction is about 1° north of the galactic plane.

The H I emission in the region around S142 is typical of regions near the Galactic plane and, therefore, has complicated H I structure made up of a large component of emission from local gas mixed with that from gas at other points along the line of sight. Most of the local component of emission is smooth in spatial structure, and can therefore be approximated by a single average spectrum over the 2° field (Fig. 3*a*). Thus, each of the line maps has had a uniform base level removed from it, corresponding to the value of this average spectrum at the relevant velocity. This operation serves the dual purpose of excluding local H I and of enhancing the dynamic range of the resulting maps. All of the H I maps shown in this paper must be considered as deviations from these base levels, and, therefore, both positive and negative map values are possible.

Inspection of Figure 3*b* reveals that in the region within about 30′ of S142 there are three velocity ranges over which the H I emission features do not change significantly. Accordingly, the first three maps shown in Figure 4 are integrations over three contiguous velocity ranges, each (more or less) delineating a single H I emission feature near S142. Of the three features (A, B, and C), feature B is most clearly related to S142. The contours on the west side of feature B follow the slope and curvature of those on the radio continuum quite accurately. Also, a general depression in the H I emission occurs near the ionizing star, extending to the northeast (see Fig. 3). The average velocity of feature B is -42 km s^{-1}, similar to that of the CO cloud.

Feature C overlaps the CO cloud and S142, itself, on the plane of the sky, but the peak emission from feature C lies slightly to the northeast of S142. It is likely that feature C is also associated with the nebula, but there is no direct, morphological evidence apart from positional coincidence. The average velocity of feature C is about 11 km s^{-1} blueshifted from that of the CO cloud. If it is associated with S142, it probably lies on the near side of the H II region (see discussion in § VIII).

Feature A is elongated and situated to the south of S142. Its average velocity is about 10 km s^{-1} redshifted from the CO cloud velocity. This feature extends outside the boundary of the 75′ map (see Fig. 3). H I features of this sort are common near the Galactic plane.

Figure 4 also shows a map of a small, high-velocity H I feature (feature X) covering part of S142. This map does not include short spacing information (spacings less than about 61λ). This feature is blueshifted by about 37 km s^{-1} from the velocity of the CO cloud. Although possibly related to S142, this low-mass feature cannot be of great dynamical significance and will not be discussed further in this paper.

The following mass determinations have been made for each of the four features illustrated in Figure 4 (assuming optically thin conditions):

$$\text{Feature A} = 2500\ M_\odot\ ,$$

$$\text{Feature B} = 1200\ M_\odot\ ,$$

and

$$\text{Feature C} = 1800\ M_\odot\ ,$$

$$\text{Feature X} = 170\ M_\odot\ .$$

These masses are determined from base levels that are carefully, but somewhat arbitrarily, chosen.

In order to put the H I features selected above into further perspective, Figure 5 shows a three-projection representation of the H I data which covers the entire velocity range shown in Figure 3. The integrated H I map on the lower left shows a ridge of H I to the east of S142 even though the range of velocities included is large.

1985ApJ...298..596J

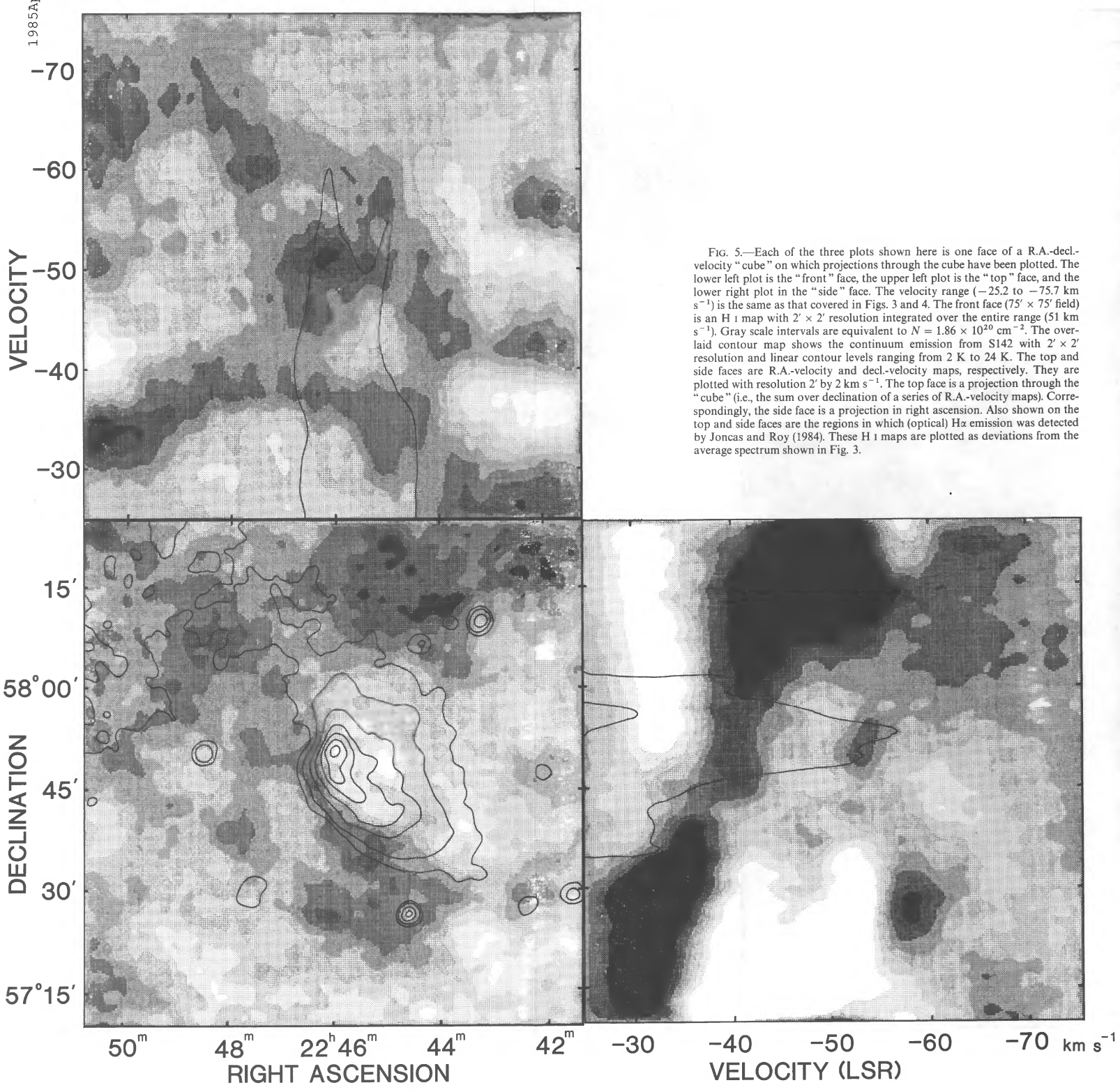

FIG. 5.—Each of the three plots shown here is one face of a R.A.-decl.-velocity "cube" on which projections through the cube have been plotted. The lower left plot is the "front" face, the upper left plot is the "top" face, and the lower right plot in the "side" face. The velocity range (−25.2 to −75.7 km s^{-1}) is the same as that covered in Figs. 3 and 4. The front face (75′ × 75′ field) is an H I map with 2′ × 2′ resolution integrated over the entire range (51 km s^{-1}). Gray scale intervals are equivalent to $N = 1.86 \times 10^{20}$ cm^{-2}. The overlaid contour map shows the continuum emission from S142 with 2′ × 2′ resolution and linear contour levels ranging from 2 K to 24 K. The top and side faces are R.A.-velocity and decl.-velocity maps, respectively. They are plotted with resolution 2′ by 2 km s^{-1}. The top face is a projection through the "cube" (i.e., the sum over declination of a series of R.A.-velocity maps). Correspondingly, the side face is a projection in right ascension. Also shown on the top and side faces are the regions in which (optical) Hα emission was detected by Joncas and Roy (1984). These H I maps are plotted as deviations from the average spectrum shown in Fig. 3.

1985ApJ...298..596J

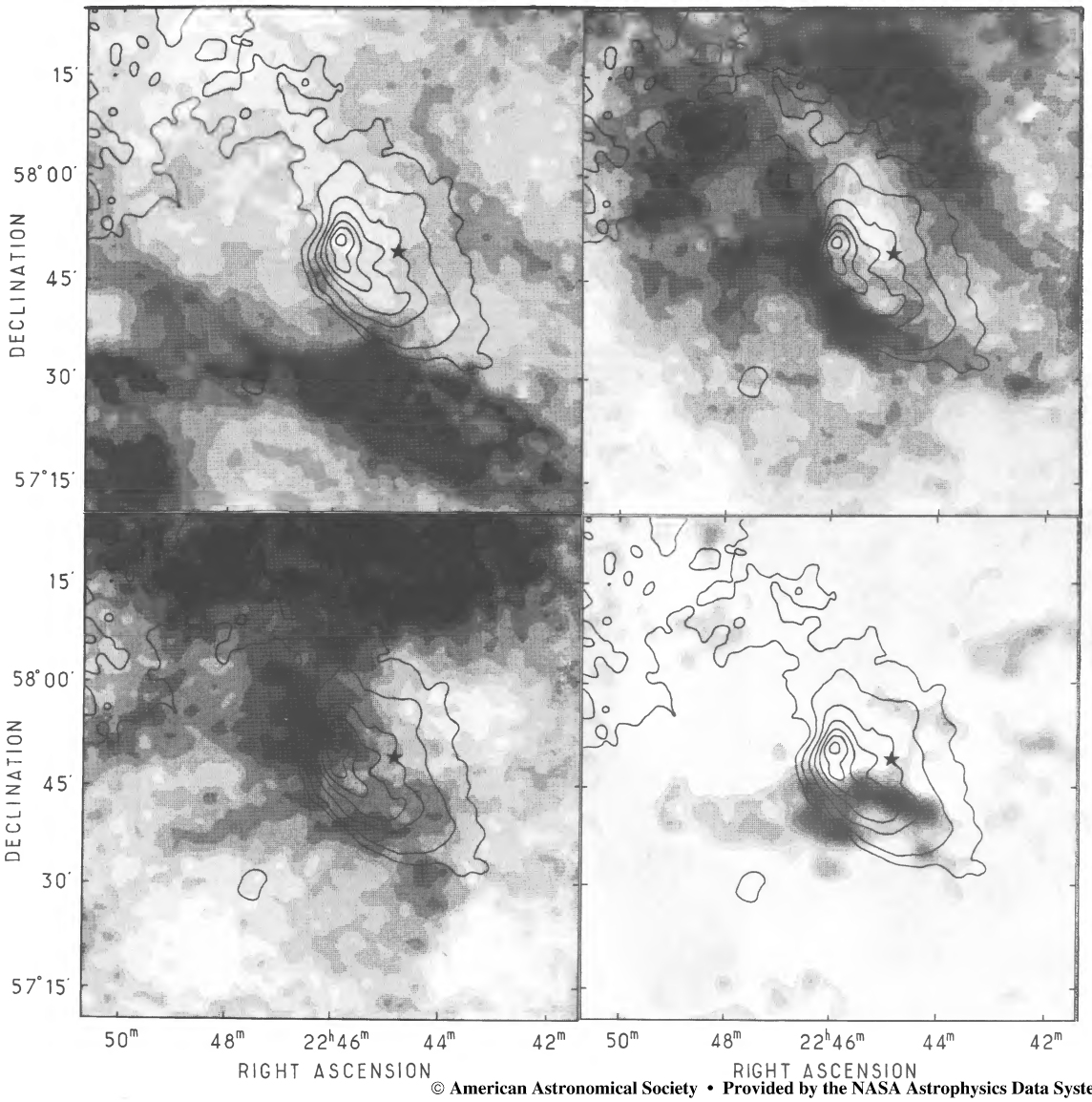

FIG. 4.—Four maps of H I emission in a 75′ × 75′ field around S142 shown with 2′ × 2′ resolution, each with overlaid continuum contours of S142. The intervals between gray levels correspond to $N = 7.6 \times 10^{19}$ cm^{-2}. The base level is the transition between the fourth and fifth gray level. The continuum contour levels range from 2 K to 24 K. Feature A (*upper left*) (−25.6 to −36.3 km s^{-1}) is a ridge of H I emission to the south of S142 which extends beyond the 75′ field; its peak column density is 5.6×10^{20} cm^{-2}. Feature B (*upper right*) (−36.6 to −47.1 km s^{-1}) is H I emission bordering the east side of S142; its peak column density is 4.3×10^{20} cm^{-2}. Feature C (*lower left*) (−47.1 to −56.9 km s^{-1}) is H I emission overlapping S142; its peak column density is 3.6×10^{20} cm^{-2}. Feature X (*lower right*) (−75.9 to −80.8 km s^{-1}) is a blue-shifted H I feature overlapping S142; its peak column density is 8.5×10^{19} cm^{-2}.

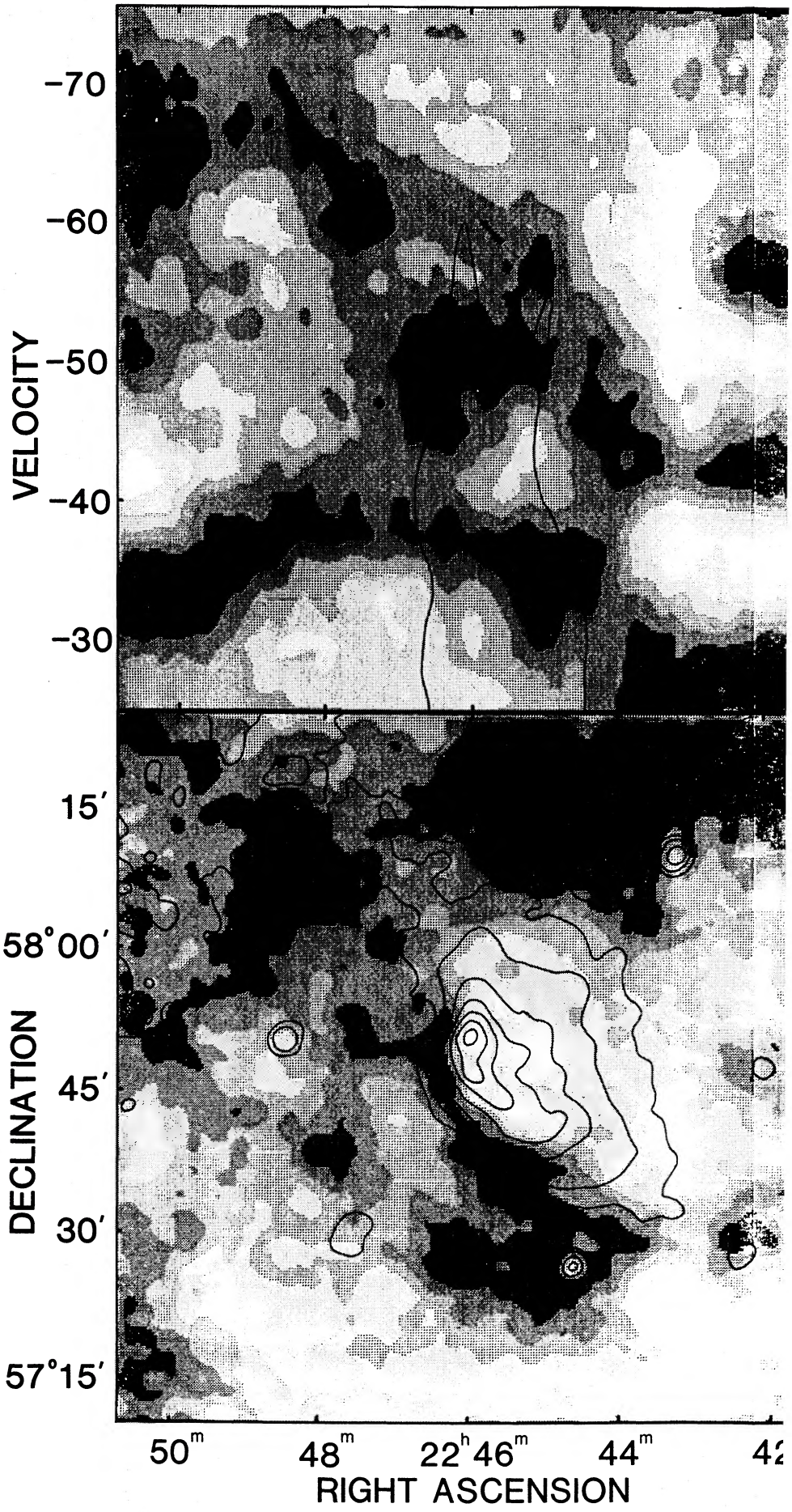

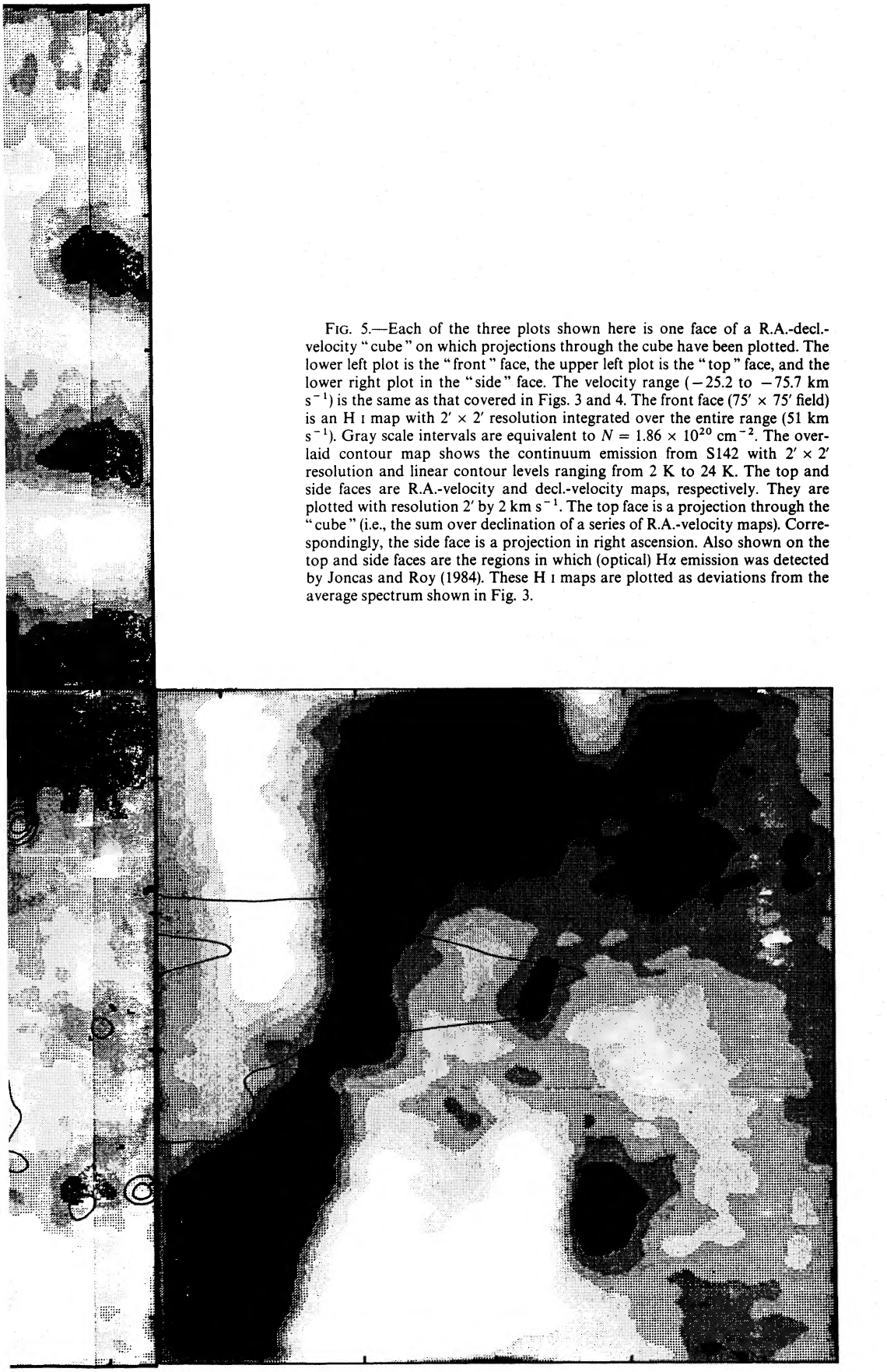

FIG. 5.—Each of the three plots shown here is one face of a R.A.-decl.-velocity "cube" on which projections through the cube have been plotted. The lower left plot is the "front" face, the upper left plot is the "top" face, and the lower right plot in the "side" face. The velocity range (−25.2 to −75.7 km s^{-1}) is the same as that covered in Figs. 3 and 4. The front face (75′ × 75′ field) is an H I map with 2′ × 2′ resolution integrated over the entire range (51 km s^{-1}). Gray scale intervals are equivalent to $N = 1.86 \times 10^{20}$ cm^{-2}. The overlaid contour map shows the continuum emission from S142 with 2′ × 2′ resolution and linear contour levels ranging from 2 K to 24 K. The top and side faces are R.A.-velocity and decl.-velocity maps, respectively. They are plotted with resolution 2′ by 2 km s^{-1}. The top face is a projection through the "cube" (i.e., the sum over declination of a series of R.A.-velocity maps). Correspondingly, the side face is a projection in right ascension. Also shown on the top and side faces are the regions in which (optical) Hα emission was detected by Joncas and Roy (1984). These H I maps are plotted as deviations from the average spectrum shown in Fig. 3.

TABLE 2

SOURCES IN S142 FIELD

No. (7P)	R.A.+ (1950)	DEC+	S(integrated)	Size	Comments
1	$22^h38^m25.0^s \pm 0.1^s$	57°17'17" ±1"	512 ± 28 mJy	1.0'x0.5' at 66°	*, BG 2238+57
2	38 50.2 ±0.8	57 19 50 ±4	30 ± 9		
3	39 14.1 ±0.5	58 42 56 ±5	54 ± 14		GT 2239+587, thermal?
4	39 56.5 ±0.2	57 11 18 ±2	124 ± 14		GT 2239+572
5	40 01.1 ±0.1	57 46 22 ±1	81 ± 6	0.8'x0.5' at 54°	
6	40 12.3 ±0.1	58 04 18 ±1	115 ± 7	0.8'x0.3' at 111°	*, GT 2240+580
7	41 06.7 ±0.4	57 40 04 ±3	21 ± 4		
8	41 33.1 ±0.1	57 29 22 ±1	61 ± 4		
9	42 05.2 ±0.1	57 47 34 ±1	29 ± 3		
10	42 08.2 ±0.4	57 42 45 ±4	10 ± 2		
11	42 09.1 ±0.2	58 27 19 ±2	31 ± 4		
12	42 15.2 ±0.3	58 50 24 ±3	72 ± 12		
13	42 23.8 ±0.2	57 27 51 ±2	30 ± 3	0.5'x0.2' at 77°	*
14	43 13.4 ±0.1	58 09 54 ±1	192 ± 10	0.6'x0.1' at 155°	*, c
15	43 35.2 ±0.1	58 35 19 ±1	240 ± 14	1.4'x0.7' at 95°	Double?, GT 2243+585
16	43 49.1 ±0.2	58 09 44 ±2	28 ± 3		
17	44 01.4 ±0.3	57 59 19 ±3	10 ± 2		
18a	44 18.8 ±0.1	58 06 48 ±1	34 ± 3		Double, c
b	44 29.0 ±0.4	58 06 31 ±2	13 ± 1		
19	44 21.0 ±0.1	56 51 41 ±1	141 ± 9	0.8'x0.4' at 44°	*
20	44 35.8 ±0.1	57 26 47 ±1	252 ± 13	0.3'x0.3'	c
21	44 46.4 ±0.2	57 47 14 ±2	33 ± 4		a, c
22	44 51.9 ±0.1	57 07 22 ±1	105 ± 6	0.6'x0.1' at 10°	*
23	45 02.2 ±0.1	56 54 55 ±2	36 ± 4		
24	45 04.1 ±0.3	58 29 26 ±2	25 ± 3		
25	45 13.0 ±0.2	57 54 07 ±3	15 ± 7		b
26	46 18.9 ±0.4	58 13 17 ±4	11 ± 2		
27	47 25.3 ±0.2	58 08 00 ±2	25 ± 2		
28	47 35.5 ±0.4	57 29 50 ±4	26 ± 3	2.3'x1.5' at 156°	*, GT 2247+575, S143
29	48 17.7 ±0.2	58 40 20 ±3	22 ± 3		Component of no. 31?
30	48 25.6 ±0.1	57 50 29 ±1	109 ± 6		c
31	48 27.0 ±0.2	58 37 47 ±2	49 ± 6	0.7'x0.4' at 31°	*
32	48 44.2 ±1.1	57 13 02 ±7	21 ± 6		
33	48 52.5 ±0.8	57 05 10 ±6	13 ± 6		
34	49 13.7 ±0.4	57 02 00 ±5	29 ± 6		
35	50 16.0 ±0.2	57 56 05 ±2	26 ± 3		
36	50 18.2 ±0.2	58 09 16 ±2	24 ± 3		
37	50 30.1 ±0.4	57 43 20 ±3	13 ± 3		
38	50 36.2 ±0.5	57 11 32 ±4	26 ± 5	0.9'x0.3' at 120°	*
39	51 02.1 ±0.2	57 50 11 ±2	39 ± 4	1.2'x0.6' at 147°	
40	51 05.2 ±0.5	57 07 54 ±4	15 ± 4		
41	51 09.3 ±0.3	57 40 29 ±3	36 ± 6		
42	51 12.4 ±0.6	57 13 18 ±6	17 ± 5	0.7'x0.4' at 128°	*
43	51 38.4 ±0.1	57 32 15 ±1	173 ± 10	0.6'x0.3' at 101°	*
44	52 07.1 ±0.7	57 41 17 ±4	24 ± 8		
45	52 13.9 ±0.3	58 17 06 ±3	23 ± 4		
46a	52 50.3 ±0.1	57 40 39 ±1	2540 ±130	0.5'x0.3' at 94°	*, BG 2252+57
b	52 42.6 ±1.3	57 41 00 ±8	270 ± 80	2.3'x1.3' at 5°	Tail?
47	53 06.9 ±0.6	57 52 37 ±2	31 ± 9		
48	53 48.6 ±0.5	58 26 21 ±2	53 ± 10		
49	53 52.6 ±0.5	57 26 31 ±4	49 ± 7	1.7'x0.9' at 139°	*
50	54 13.4 ±0.1	58 15 14 ±1	479 ± 27	1.0'x0.7' at 60°	*, S 148

NOTES.—Symbols are as follows. +: Positional errors are formal fitting errors. Uncertainties due to bandwidth "smearing" are not included. *: Observed source shapes may be largely due to bandwidth "smearing." a: This source does not appear in the map of Israel 1977 but has probably been removed before plotting. b: This source is not listed by Israel 1977 but is visible in his map of S142. c: This source is listed by Israel 1977 as being in his S142 field. Sources are as follows. BG: Fanti *et al.* 1974. GT: Taylor and Gregory 1983. S: Sharpless 1959.

The right face of Figure 5 shows two large emission features. The one at -30 km s^{-1} is feature A integrated approximately along its length. The one north of declination 58° at -48 km s^{-1} is the large emission region north of S142 (see Fig. 3). Since this feature also has a large east-west extent, it will be bright on the decl.-velocity map. The gap between these two components is at -41 km s^{-1}, the systemic velocity of the H I–H II–CO complex. Feature C can also be seen near the center of the side face at a velocity of -52 km s^{-1}.

The upper face of Figure 5 has a central peak at about -50 km s^{-1}. This peak results from the projection of feature C which has little velocity variation in the north-south direction.

For comparison of optical and H I line velocities, Figure 5 also shows (on the upper and right faces) the range of velocities and positions for which Hα emission was detected by Joncas and Roy (1984). However, this distribution has been truncated, and about 20% of the velocity points, more positive than -25.2 km s^{-1}, are missing.

V. MOLECULAR GAS NEAR S142

Figure 6 shows a map of ^{12}CO superposed on the continuum map of S142. The map was produced by Israel (1980) with 8.'0 resolution and contains a single peak of apparent brightness temperature adjacent to the steepest edge of the continuum brightness just to the north of the continuum peak. The ^{12}CO peak is at an LSR velocity of -42.8 km s^{-1}, and there is a similar ^{13}CO peak (4′ to the southwest) at -41.1 km s^{-1} where a secondary ^{12}CO peak is present. Israel estimates the total mass of molecular material in the cloud to be about 200 $M_\odot$ using the relation $N(H_2) = 5 \times 10^5 N(^{13}CO)$ developed by Dickman (1978). This relation must be used with caution (it has recently been revised by Frerking, Langer, and Wilson 1982), being based on the assumption that ^{13}CO is optically thin. There may also be fractionation effects for ^{13}CO because of the photon excitation from the star (McCutcheon *et al.* 1980; Penzias 1983). However, the cloud is small, and the relation is probably valid. The peak column density of ^{13}CO is $\sim 4.5 \times 10^{15}$ cm^{-2}, corresponding to an H_2 column density of 2.3×10^{21} cm^{-2} and thus a density of ~ 200 H atoms cm^{-3} in the core of the molecular cloud, for an assumed size of ~ 7 pc.

Assuming that this cloud, albeit small, is the remnant of the progenitor molecular cloud for the stars in NGC 7380, the velocity of -41 km s^{-1} provides a good estimate of the "rest velocity" for the H II–H I–H_2 complex being studied here.

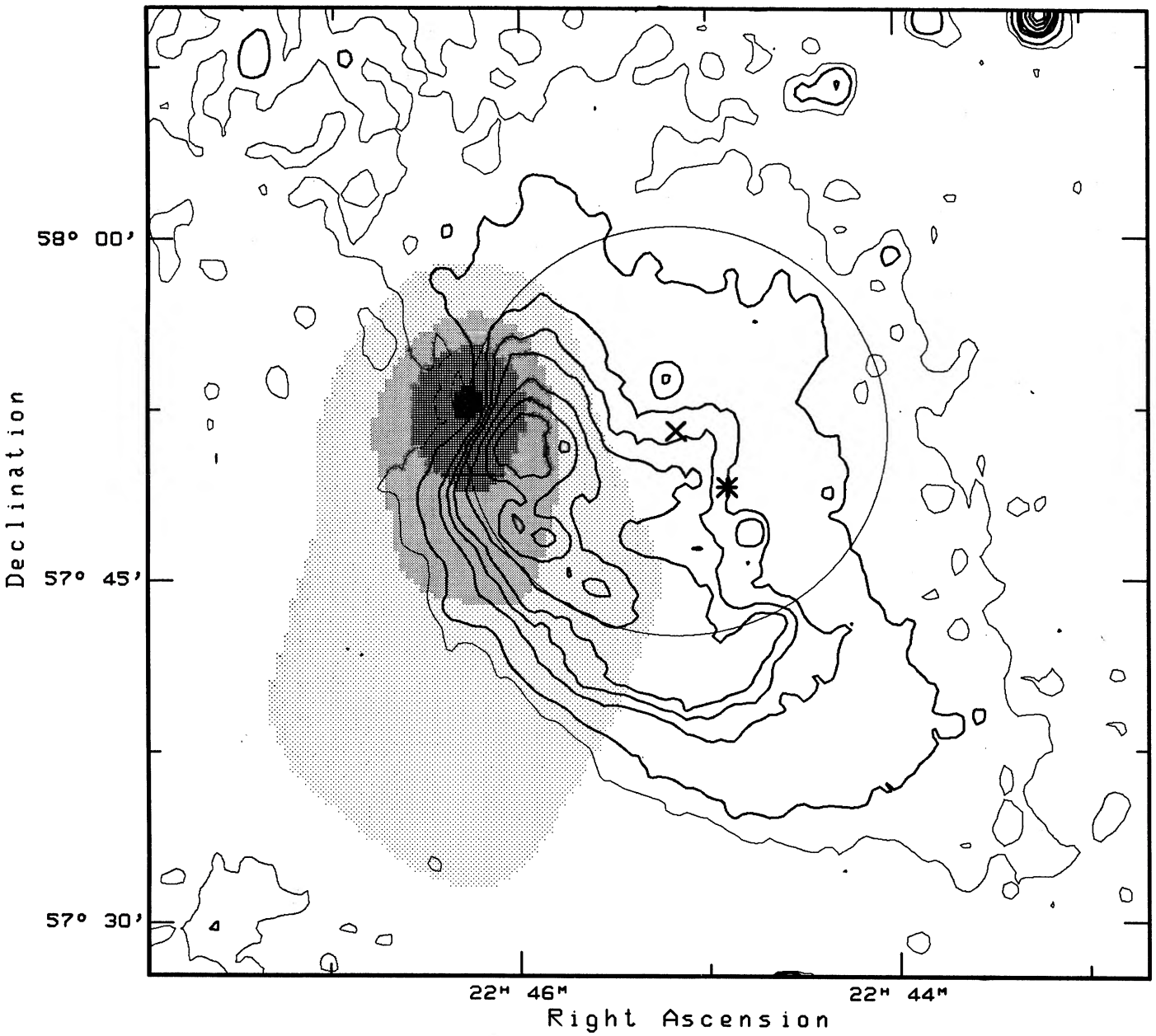

FIG. 6.—A superposition of the CO map of the molecular cloud (Israel 1980) on the radio continuum map. Also shown are the position of DH Cephii (*star symbol*), the position of the center of NGC 7380 (*cross symbol*) and the radius of the cluster (*circle*) (Baade 1983). The CO map, integrated over velocity, is contoured in steps of 2.6 K of T_A*. The continuum contours are 2, 3, 6, 8, 10, 14, 18, and 22 K.

VI. DISSOCIATED HYDROGEN

Figure 7 is a plot showing a radial profile of continuum emission and H I emission taken from the map of feature B, both averaged over a 90° sector centered on DH Cep. A local minimum of H I emission is present near the star, and the column density rises from there by about 5.25×10^{20} cm^{-2} on the ridge of feature B, falling again by about half the original rise. The depression in H I column density is roughly coincident with the region around the star. The continuum emission falls off to half intensity at a radius of about 11 pc, just at the start of the rise in H I column density in the ridge of feature B. The ridge is about 5 pc thick in profile. The interpretation suggested by this data is that the depression in the H I column density around DH Cep is caused by the fact that most of the gas is ionized, and the ridge of feature B is dissociated molecular material. Although the ridge gas is the most easily recognized, the gas around feature B, and possibly most of feature C is also dissociated gas.

In order to shed more light on the relationship between feature B, feature C and the ionized gas, the intensity of H I emission was averaged over a 10′ wide strip centered on the continuum peak and is shown as an R.A.-velocity plot in Figure 8. Feature B can be seen near -40 km s^{-1}, and feature C, near -52 km s^{-1}. The H II region, whose location is indicated by a profile of continuum brightness, seems partly wrapped by an H I shell composed of both features. As indicated by the optical observations (Paper I) and the lack of H I emission in its vicinity, S142 is open to the interstellar medium on its western side and away from the observer. Feature C is blueshifted by an average of 11 km s^{-1} from the CO cloud velocity, it would be the "face-on" part of the shell, located on the near side of the H II region, and expanding toward the observer. Feature B is the eastern part of the shell and is closely linked to the molecular cloud.

Because of the confusion with extraneous Galactic H I, the amount of dissociated gas cannot be accurately described. The mass of "missing" gas in the depression (below the average line shown in Fig. 7) is about 900 $M_\odot$ including the three quadrants not shown in Figure 7. Since this has been estimated only from the map of feature B, it is probably an underestimate.

The amount of gas in the "ridge" (Fig. 7) is about 250 $M_\odot$. This certainly represents a lower limit to the amount of dissociated gas. Other estimates (from the maps in Fig. 4) are as follows: (*a*) All of feature *B* (lower base level than for Fig. 6) is 1200 $M_\odot$. (*b*) Feature B plus feature C is 3000 $M_\odot$.

The following equilibrium relation has been successfully used to model dissociation zones around H II regions (see Roger and Irwin 1982 for a summary);

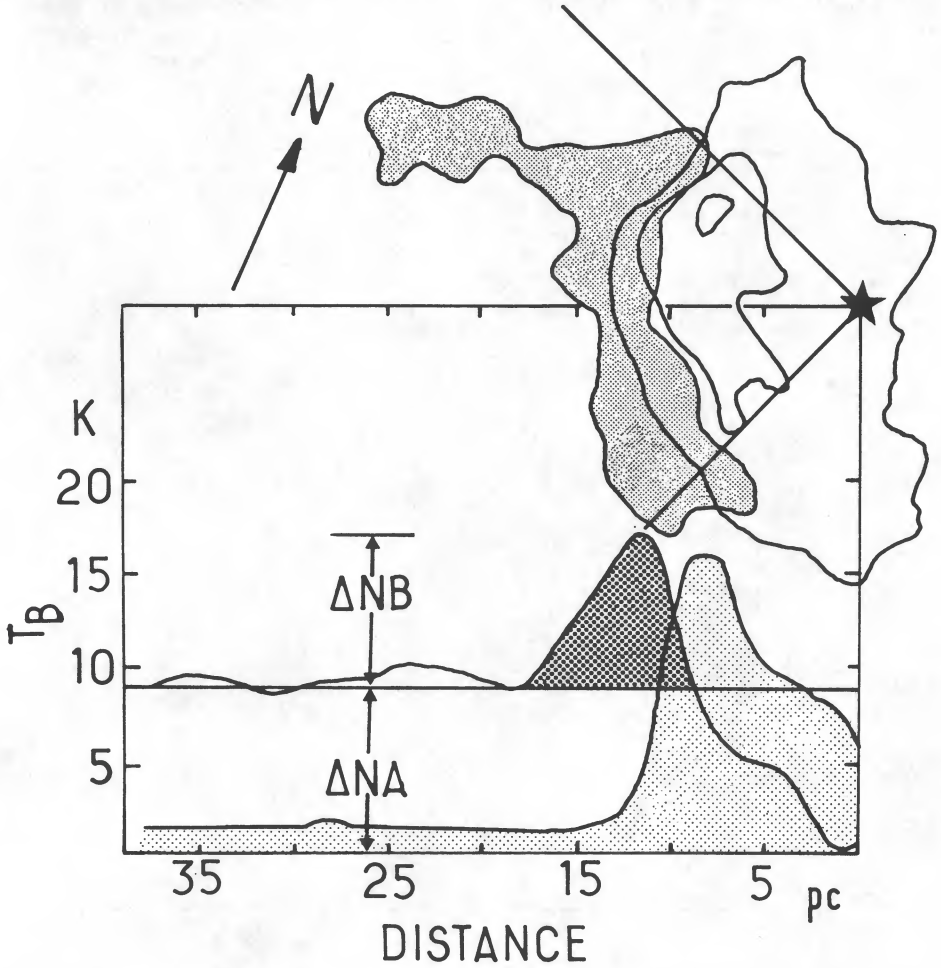

FIG. 7.—Radial profiles of radio continuum brightness temperature (*lower*) and H I column density (*upper*). The profiles are averaged over a 90° sector whose average position angle is 113° and whose apex is at the position of DH Cep. The profile cut is shown relative to the continuum emission (*contours*) and adjacent H I emission (*shaded contour*) taken from the map of feature B. The H I "depression" ($\Delta N_A = 2.5 \times 10^{20}$ cm^{-2}) is defined as the amount of gas "missing" below the level shown on the H I profile. The H I "ridge" ($\Delta N_B = 2.8 \times 10^{20}$ cm^{-2}) is defined as the shaded portion of the H I profile.

$$n_{H_2} = \frac{Rn_t^2}{2Rn_t + I_0(r_0/r)^2 \beta N_{H_2}{}^{-1/2} e^{-kN_t}}, \quad (1)$$

where $n_t = n_{H\,I} + 2n_{H_2}$ relates the total, atomic, and molecular gas number densities, and N_t and N_{H_2} are corresponding column densities along radii, r, from the star. R is the molecular formation rate; I_0 is the dissociation rate at a radius r_0, the radius of the ionization boundary; and k is the dust absorption coefficient. The term $\beta N_{H_2}{}^{1/2}$ accounts for self-shielding of the Lyman band absorption in the square root portion of the curve of growth where $\beta = 4.2 \times 10^5$ cm^{-2} (Jura 1974). This relation can be found by setting $\delta n_{H_2}/\delta_t = 0$ in equation (A1) of Hill and Hollenbach (1978).

From Figure 7, r_0 is taken as 10.9 pc, the point at which continuum emission drops to half its peak intensity. At this distance I_0 can be scaled from the table of photoabsorption rates given in Hollenbach, Chu, and McCray (1976) and is taken in this case to be 2.87×10^{-9} s^{-1}. The coefficient k is taken to be 3×10^{-21} cm^2 (Bohlin 1975; York *et al.* 1973) and R, 3×10^{-17} cm^3 s^{-1} (Jura 1974, 1975). A numerical integration of equation (1) for a total hydrogen density of 100 cm^{-3} yields an H I shell which is 3.4 pc thick, in reasonable agreement with the thickness of the "ridge." The total mass of H I in a spherically symmetric shell would be about 15,000 $M_\odot$. However, since the observed shell covers only about one-eighth of the sphere, the total mass is expected to be about 1900 $M_\odot$.

A guide to the time scale, t_{eq}, at which dissociation equilibrium is reached for a particular distance, x, from the ionization boundary is given by Hill and Hollenbach (1978) as $t_{eq} = x/(4Rnx_{1/2})$, where $x_{1/2}$ is the distance from the ionization boundary to the point at which the gas is half-molecular in equilibrium. R and n are as given in equation (1), and planar geometry is assumed. For $x = x_{1/2}$, t_{eq} is about 3×10^6 yr. Assuming the age of S142 to be 2×10^6 yr, the dissociation zone in feature B should have had almost enough time to reach theoretical equilibrium.

VII. A COMPARISON WITH A SIMILAR H II REGION, NGC 281

The most similar H II region for which H I observations have been made is NGC 281 (Roger and Pedlar 1981). NGC 281 (S184) is more displaced from the Galactic plane than S142, and associated H I is easier to separate from the "field H I" around it. Table 3 is a comparative list of various features of the two regions. Both H II regions are ionized by stars of similar spectral type. Judging from the ages given for the associated star clusters, S142 appears to be a somewhat more evolved system, although its peak emission measure is higher than that for NGC 281. The derived densities and total masses of ionized gas are within a factor of 2 of each other. The greatest difference between these two systems lies in the amount of associated molecular gas. The CO cloud associated with S142 is startingly small compared with the size of the CO cloud near NGC 281. The size of the CO cloud in the NGC 281 complex is more typical of those associated with bright H II regions. It also contains an H_2O maser. Although no known H_2O maser

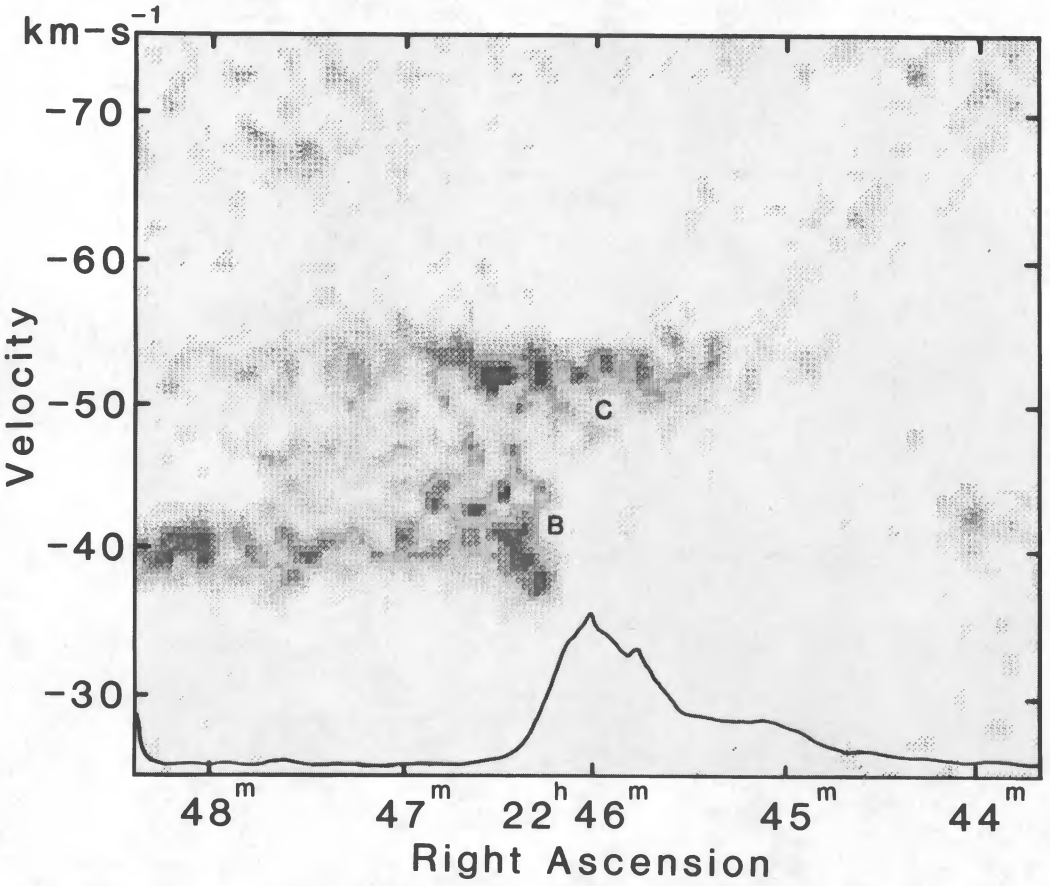

FIG. 8.—A plot of R.A. vs. velocity averaged over a strip 10′ wide, centered on the continuum peak. The range of brightness temperature (above and below the reference spectrum) is ±9 K. A profile of continuum brightness in the same strip is shown as a reference. Part of features B and C are indicated by "B" and "C," respectively. Together they show some "wrapping around" the H II region that might be expected from dissociated H I.

TABLE 3

A COMPARISON OF OBSERVED AND DERIVED PARAMETERS FOR S142 AND NGC 281

Parameter	S142	NGC 281
l, b	107°, −1°	123°, −6°
Exciting star	O6 V + O6 V	O6.5 V + O8 V
H II:		
Derived mass ($M_\odot$)	4000	2200
Peak emission measure (cm^{-6} pc)	16000	6200
Derived peak density (cm^{-3})	65	47
Size (pc)	14 × 6	13 × 7
H I:		
Peak column density (cm^{-2})	4×10^{20}	8×10^{20}
Mass ($M_\odot$)	3000	3500
Molecular:		
Peak column density (cm^{-2})	2.3×10^{21}	1.6×10^{22}
Mass ($M_\odot$)	200	4000
Age of associated stars (yr)	2×10^6	1×10^6
OH maser	no	no
H_2O maser	?	yes

exists near S142, it is unlikely that a search has been made. Both regions have been searched for OH masers, but no maser sources were found (Turner 1969).

A broad region of enhanced H I, containing about 3500 $M_\odot$, partly surrounds NGC 281. This partial shell, with a derived size of ~8 pc, contains gas with a density of ~20 cm^{-3}, and is expanding at about 6 km s^{-1} relative to the CO cloud. As discussed in § VIII, this shell bears a strong resemblance to features B and C.

The geometry of the two systems happens to be different. In NGC 281 the ionizing star is near the middle of the H II region, and the neutral material is on the front face of the nebula. In S142 the juxtaposition of the CO cloud, H I features, H II region, and ionizing star is largely transverse to the line of sight.

VIII. DISCUSSION

In this section we will present a summary of the optical and radio observations and attempt to derive a consistent geometrical picture of the S142 complex. We will emphasize large-scale features which are (possibly) important enough to be "generalized" as statements of the characteristics of H II regions at this stage of development.

The major observed features of this complex include the following and are shown primarily in Figures 2, 4, and 6.

NGC 7380.—This feature is a young open cluster containing about 192 stars including DH Cephii and several other early-type stars. The diameter of the cluster is about 18′ (Baade 1983). There is a total of at least 440 $M_\odot$ in the form of stars (Moffat 1971).

S142.—This feature is an H II region, delineated by the radio continuum observations presented in this paper. The total mass of ionized material (derived from a model) is about 4000 $M_\odot$. The radial component of flow velocity in the H II region is defined by the optical Hα (Paper I) in regions that are not affected by obscuration. The flow is redshifted over most of the nebula but is blueshifted near the radio continuum peak.

A molecular cloud.—This feature is revealed by CO observations (Israel 1980). The position of the cloud core (Fig. 6) is adjacent to the radio continuum peak. Its mass is about 200 $M_\odot$. The velocity of the cloud is taken as the systemic velocity of the complex, and all velocities in this discussion are given relative to this velocity (−41 km s^{-1}). (Because the mass of the molecular cloud is so small, a better rest frame would be provided by the average velocity of the cluster members, but sufficiently accurate data of this sort is not known to be available.

H I *features B and C.*—These features are delineated by H I line observations. Feature B is adjacent to the eastern edge of the H II region and has an average velocity of −1 km s^{-1}. Feature C is assumed in this discussion to be associated with the complex. Its position is similar to that of feature B but overlaps the ionized region more in the line of sight and has an average velocity of about −11 km s^{-1}. The boundaries of these features are difficult to determine precisely, but each appears to have a mass of about 1000–2000 $M_\odot$.

A local minimum in Galactic H I *emission.*—The size of the minimum is comparable to that of the ionized region and is displaced slightly to the west.

DH Cephii.—This feature is a pair of O6 V stars, capable of generating about 3.5×10^{49} ionizing photons per second.

Optical obscuration.—This feature exists in bands which appear to project from the area east of the nebula. In particular, the region around the peak of the radio continuum is heavily obscured. The average "excess" visual extinction (derived from Table 1; Moffat 1971) is 0.6 mag for the cluster members.

There are several other observational points which affect the detailed interpretation.

1. Two early-type stars, an O9 and an O9.5 (Fig. 2), are associated with bright patches of Hα emission and bright rims. Together they contribute about 9% of the total available ionizing photon flux. However, they are relatively more important for dissociation of H_2, contributing about 25% of the dissociating photons. Several early B stars in the cluster may contribute a few more percent.

2. A trough in the radio continuum emission cutting into the western side of the H II region is coincident with a similar trough in Hα emission (Fig. 2).

From this body of information it seems certain that the star formation process which produced NGC 7380 took place (or ceased) fairly recently. (Baade 1983 argues against strict coeval star formation for NGC 7380.) However, the complex is old enough that vestiges of the progenitor material remain only in the region least affected by the several early-type stars that have formed. We can assume that the bulk of the progenitor cloud was originally located near the cluster center as shown in Figure 6.

Nearly all the gaseous material in the progenitor cloud, which is assumed originally to have been molecular, is now either ionized or dissociated. The total gaseous mass present in

the region, $\sim 7000\ M_\odot$, forms a lower limit to the mass of the progenitor cloud. Higher density, neutral gas on the eastern side of the cluster forms an ionization boundary for S142, the H II region. Most of the neutral, gaseous material is atomic, and only about 200 $M_\odot$ of molecular material remains in a "core region" (Fig. 6). The atomic gas forms a partial "shell" comprised of H I features B and C in this paper which surround the H II region on the east and front sides. The gas in feature C is moving toward us with a velocity of about 11 km s^{-1}, probably representing the expansion velocity of the whole gaseous complex (except, perhaps, the molecular cloud core). The densities of the gaseous material are not extremely high, probably $\sim 10^2$ cm^{-3} in the neutral gas, and about 60 cm^{-3} (maximum) in the ionized gas. Since the core of the molecular cloud seems particularly robust against ionization/dissociation, its density may be much higher. High-resolution molecular line observations would be needed to confirm this.

The west side of the H II region is open to the interstellar medium. In fact, the dearth of H I in this region indicates that it has been swept clear. The Hα velocity measurements (Paper I) indicate flow from east to west as well as away from the observer. The overall picture, illustrated in Figure 9, is one of a partial shell of neutral material feeding the H II region. The ionized gas is expanding away from the shell into a tenuous region to the west and on the back side of the nebula.

This picture is similar to the theoretical "champagne" models of Tenorio-Tagle (1979, 1982) who has considered the development of H II regions on the edges of molecular clouds. The champagne phase occurs when the ionization front breaks out into the low-density, intercloud medium. Although we are unable to make strict quantitative comparisons, the present observations fit these models qualitatively. In particular, our observations are in keeping with the exponential decline in density predicted in a well-developed champagne flow.

The general picture described so far is complicated by several of the observational points made earlier in this section. The trough in the radio continuum emission seems to require the addition of some sort of "spur" of dark material protruding into the main ionized cavity, shown schematically in Figure 9. The size of the spur shown in Figure 9 may not quite explain the depth of the trough in the radio continuum, and the "spur" could actually be a sheet of molecular material at an angle to the line-of-sight. However, because of projection ambiguities, it is difficult to portray in the third dimension.

There may also be small ionized cavities associated with the late O stars. Since one of them is close to the region of heavy obscuration around the continuum peak, it may be responsible for local flows of material towards the observer. The [N II] line splitting observed by Johnson, Mack, and Songsathaporn (1982) is probably the combined result of flow from the "spur" plus flow from the foreground shell (feature C in H I). Johnson *et al.* found two [N II] components over most of the eastern portion of S142 with a velocity separation of about 30 km s^{-1}.

Using a total mass of stars as 440 $M_\odot$ (Moffat 1971), and our estimate of about 7000 $M_\odot$ of gas in the region, the derived star formation efficiency is about 6% for the cluster. This is somewhat lower than that predicted for simple virial models of bound clusters (Mathieu 1983). Uncertainties in this number could be quite large, however, since the number of stars in NGC 7380 has been revised from 45 to 192 by Baade (1983), tending to increase the efficiency. Also, the gas in this complex is highly processed, and the initial mass of the star forming region is consequently difficult to estimate.

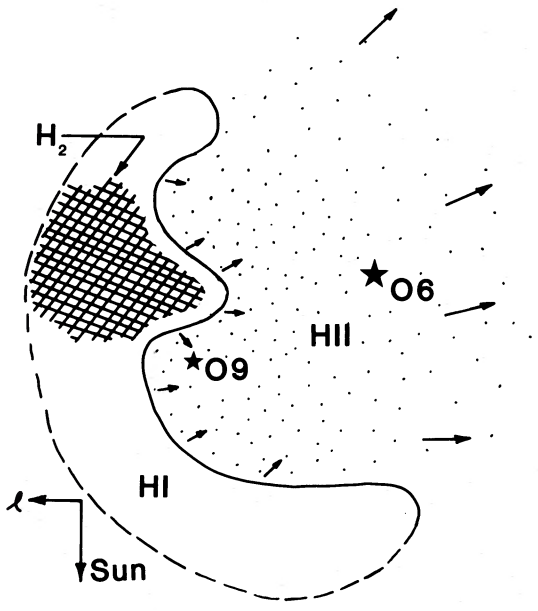

FIG. 9.—A pictorial representation of the NGC 7380/S142 complex showing the various gas components, the ionizing star (DH Cephii) and an O9 star. The shell-like region is mostly atomic except for the cross-hatched area which is molecular. The region inside the shell is ionized. The relative size of the cluster can be inferred from Fig. 8.

IX. CONCLUSION

NGC 7380 is a young open cluster, the result of star formation which terminated some 2×10^6 yr ago when several O-type stars formed, causing the dispersal of the progenitor cloud. Dispersal is not yet complete, however, and the region still contains a large quantity of gas, most of which is now in ionized and atomic form. A small quantity of molecular material also remains in a region of somewhat higher density. The cluster has an unusually large number of members and seems to have a deficit of stars near the center. This indicates that the cluster may be young enough that it has not yet been stripped of its weakly bound members (Baade 1983).

The suggested configuration of the ionized and atomic gas is a partial shell of H I surrounding the H II region S142. The masses of ionized and neutral gas are 4000 $M_\odot$ and 3000 $M_\odot$, respectively. H I is being ionized by the O star, DH Cep, and is flowing generally toward a region of low density on the other side of the star. The H I itself is the result of the photodissociation of H_2 in the progenitor molecular cloud. The dissociation front seems to have progressed through most of the cloud, leaving only a small molecular cloud of about 200 $M_\odot$. The total mass of stars is about 6% of the original mass of progenitor gas.

The Dominion Radio Astrophysical Observatory is operated as a national facility by the National Research Council of Canada. We thank C. R. Purton for a critical reading of the manuscript.

REFERENCES

Baade, D. 1983, *Astr. Ap. Suppl.*, **51**, 235.
Baars, J. W. M., Genzel, R., Pauliny-Toth, I. I. K., and Witzel, A. 1977, *Astr. Ap.*, **61**, 99.
Blitz, L., Fich, M., and Stark, A. A. 1982, *Ap. J. Suppl.*, **49**, 183.
Bohlin, R. C. 1975, *Ap. J.*, **200**, 402.
Dickman, R. L. 1978, *Ap. J. Suppl.*, **37**, 407.
Fanti, C., Felli, M., Ficarra, A., Salter, C. J., Tofani, G., and Tomasi, P. 1974, *Astr. Ap. Suppl.*, **16**, 43.
Felli, M., and Churchwell, E. 1972, *Astr. Ap. Suppl.*, **5**, 369.
Felli, M., Harten, R. H., Habing, H. J., and Israel, F. P. 1978, *Astr. Ap. Suppl.*, **32**, 423.
Felli, M., Tofani, G., Fanti, C., and Tomasi, P. 1977, *Astr. Ap. Suppl.*, **27**, 181.
Frerking, M. A., Langer, W. D., and Wilson, R. W. 1982, *Ap. J.*, **262**, 590.
Garay, G., and Rodríguez, L. F. 1983, *Ap. J.*, **266**, 263.
Georgelin, Y. M. 1975, Thèse de doctoral d'état, Université d'Aix-Marseille.
———. 1985, private communication.
Hill, J. K., and Hollenbach, D. J. 1978, *Ap. J.*, **225**, 390.
Hollenbach, D. J., Chu, S. I., and McCray, R. 1976, *Ap. J.*, **208**, 458.
Humphreys, R. M. 1978, *Ap. J. Suppl.*, **38**, 309.
Israel, F. P. 1977, *Astr. Ap.*, **60**, 233.
———. 1980, *A.J.*, **85**, 1612.
Johnson, P. G., Mack, P., and Songsathaporn, R. 1982, *Ap. Space Sci.*, **86**, 331.
Joncas, G., and Roy, J.-R. 1984, *Ap. J.*, **283**, 640 (Paper I).
Jura, M. 1974, *Ap. J.*, **191**, 375.
———. 1975, *Ap. J.*, **197**, 575.
Kallas, E., and Reich, W. 1980, *Astr. Ap. Suppl.*, **42**, 227.
Mathieu, R. D. 1983, *Ap. J. (Letters)*, **267**, L97.
McCutcheon, W. H., Dickman, R. L., Shuter, W. L. H., and Roger, R. S. 1980, *Ap. J.*, **237**, 9.
Moffat, A. F. J. 1971, *Astr. Ap.*, **13**, 30.
Panagia, N. 1973, *A.J.*, **78**, 929.
Pedlar, A. 1980, *M.N.R.A.S.*, **192**, 179.
Penzias, A. A. 1983, *Ap. J.*, **273**, 195.
Roger, R. S., and Irwin, J. A. 1982, *Ap. J.*, **256**, 127.
Roger, R. S., and Pedlar, A. 1981, *Astr. Ap.*, **94**, 238.
Roy, J.-R., and Joncas, G. 1985, *Ap. J.*, **288**, 142.
Sharpless, S. 1959, *Ap. J. Suppl.*, **4**, 257.
Taylor, A. R., and Gregory, P. C. 1983, *A.J.*, **88**, 1784.
Tenorio-Tagle, G. 1979, *Astr. Ap.*, **71**, 59.
———. 1982, in *Regions of Recent Star Formation*, ed. R. S. Roger and P. E. Dewdney (Dordrecht: Reidel), p. 1.
Turner, B. E. 1969, *A.J.*, **74**, 985.
Warner, J. W., and Black, J. H. 1978, *A.J.*, **83**, 586.
Weaver, H., and Williams, D. R. W. 1973, *Astr. Ap. Suppl.*, **8**, 1.
Williams, D. R. W. 1973, *Astr. Ap. Suppl.*, **8**, 505.
York, D. G., Drake, J. F., Jenkins, E. B., Morton, D. C., Rogerson, J. B., and Spitzer, L. 1973, *Ap. J. (Letters)*, **182**, L1.

P. E. Dewdney and L. A. Higgs: Dominion Radio Astrophysical Observatory, P.O. Box 248, Penticton, B.C. V2A 6K3, Canada

G. Joncas: Observatoire de Marseille, 2 Place Le Verrier, 13248 Marseille Cedex 4, France

J. R. Roy: Département de physique, Université Laval, Québec, P.Q. G1K 7P4, Canada